Correlation of structural and Johari–Goldstein relaxations in systems vitrifying along isobaric and isothermal paths

2007 J. Phys.: Condens. Matter 19 205133

(http://iopscience.iop.org/0953-8984/19/20/205133)

IOP PUBLISHING JOURNAL OF PHYSICS: CONDENSED MATTER

J. Phys.: Condens. Matter **19** (2007) 205133 (10pp) doi:10.1088/0953-8984/19/20/205133

Correlation of structural and Johari–Goldstein relaxations in systems vitrifying along isobaric and isothermal paths

S Capaccioli[1,2,4], **K Kessairi**[1,3], **D Prevosto**[1,3], **M Lucchesi**[1,3] **and P A Rolla**[1,3]

[1] Dipartimento di Fisica, Università di Pisa, Largo B. Pontecorvo 3, I-56127, Pisa, Italy
[2] CNR-INFM, CRS SOFT, Piazzale Aldo Moro 2, 00185, Roma, Italy
[3] CNR-polyLab, Largo B. Pontecorvo 3, I-56127, Pisa, Italy

E-mail: capacci@df.unipi.it

Received 11 October 2006
Published 25 April 2007
Online at stacks.iop.org/JPhysCM/19/205133

Abstract

The effect of isobaric cooling (over the range 190–350 K) and isothermal compression (up to 700 MPa) on structural α- and secondary β-relaxations has been studied for low molecular weight glass-forming systems. The shape of the α-loss peak was found to change with temperature T and pressure P but to be constant for a combination of T and P giving the same $\tau_\alpha(T, P)$. The invariance of shape at constant $\tau_\alpha(T, P)$ involved also the excess wing, i.e. the process showing up at the high-frequency tail of the α-loss peak in systems with no well-resolved β-process. Likewise, systems where the excess wing evolved to a well-resolved β-peak showed that the timescale of the β-process was strongly related to that of the α-peak. Also in this case, once a given value $\tau_\alpha(T, P)$ was fixed, a corresponding value $\tau_\beta(T, P)$ was found for different T and P. Same results were found also for a binary mixture of a polar rigid molecule dissolved in an apolar solvent, i.e. a model system for Johari–Goldstein intermolecular relaxation. These evidences imply that a strong correlation exists between structural α- and Johari–Goldstein relaxation over a wide interval of temperature and density.

(Some figures in this article are in colour only in the electronic version)

1. Introduction

Glassy systems are characterized by an universal, ubiquitous phenomenon: the secondary β-relaxation, a local process active in the glassy state [1]. Among the various types of

[4] Author to whom any correspondence should be addressed.

secondary relaxation, the intermolecular one, known as Johari–Goldstein (JG), entails motions of essentially all the parts of the molecules and it is expected to be related to the structural and cooperative α-relaxation [2]. The JG β-relaxation can be singled out and identified due to the sensitivity of its timescale to applied pressure, much stronger than that shown by relaxation due to intramolecular degrees of freedom [3]. The possibility of classifying the secondary β-relaxation and determining its origin on the basis of dynamic properties has been shown in [3–5]. The isothermal reduction of volume caused by the application of pressure slows down both structural and secondary dynamics with different dependence, in a similar way to what happens for isobaric cooling. Among the various models in the literature explaining the divergence of τ_α with isobaric cooling, the free volume [6] and the Adam and Gibbs [7] model can be mentioned, relating the slowing down to the reduction of unoccupied volume and configurational entropy, respectively. Also an isothermal compression (i.e. a decrease of specific volume v) reduces both the unoccupied volume and the configurational entropy, thus slowing down the structural relaxation. Extensions of both the free volume [8] and Adam–Gibbs [9] models to consider the effect of hydrostatic pressure have recently been proposed. Recently, it has been shown [10, 11] that the behaviour of relaxation times $\tau_\alpha(T, v)$ for different T and v collapses to a master curve when plotted versus Tv^γ, with γ a material constant related to the steepness of the intermolecular repulsive potential [10] or to thermodynamic properties of the system [12]. Although various theories of the glass transition face the problem of understanding the cause of the slowing down of the structural dynamics, usually the physical mechanism underlying the β-relaxation is neglected and no general prediction for the T–P dependence of τ_β has been proposed until now. The JG β-relaxation is often considered as an unrelated (and not relevant) process, despite the fact that, due to its intermolecular nature, its correlation to the structural α-relaxation should be expected and indeed has been recently demonstrated by means of an NMR experiment [13]. Few exceptions can be found in some enlightening and excellent papers over the past decades. In their pioneering papers, Johari and Goldstein said that 'molecular mobility seen as β-relaxation is intrinsic to the nature of the glassy state' and suggested a specific model for the intermolecular β-mechanism [2]. Later on, correlations between α- and β-dynamics have been reported by different groups (e.g. [26–28]).

Another weak point of the above-quoted theories of the glass transition is the lack of predictions concerning the dispersion (time or frequency dependence) of the structural relaxation and its evolution when $\tau_\alpha(T, P)$ varies over orders of magnitudes. Usually, the dispersion and τ_α are obtained independently as separate and/or unrelated predictions and it is unlikely that, when $\tau_\alpha(T, P)$ is constant for different combinations of T and P because of compensating effects on the molecular mobility, the dispersion scales in the same way. Such approaches appear to be incompatible with experimental evidence recently pointed out for various glass-formers [14]: for a given material at a fixed value of $\tau_\alpha(T, P)$, the dispersion is constant, independent of thermodynamic conditions (T and P). In other words, the shape of the relaxation function does not depend on T or P separately, but only on the relaxation time: for example, if the structural relaxation function is represented by a Kohlrausch–Williams–Watts (KWW) function, $\Phi(t) = \exp[-(t/\tau_\alpha)^{\beta_{\mathrm{KWW}}}]$, then the stretching parameter β_{KWW} is a direct function only of τ_α, i.e. $\beta_{\mathrm{KWW}}(\tau_\alpha)$, an unlikely result if dispersion and τ_α were mutually independent. Such evidence, found by means of dielectric spectroscopy in [14], was also confirmed for a number of glass-forming systems by using other techniques, like light scattering or NMR [1]. Among the various theoretical approaches considering both slow and fast relaxation dynamics, only the coupling model [15, 16] predicts a correlation between the α-dispersion and the timescale of α- and β-relaxation. In fact, if the JG β-process is identified with the primitive relaxation of the coupling model (CM), a local motion the precursor of the α-relaxation [3, 16], due to many-molecule dynamics its timescales $\tau_{\mathrm{JG}} \approx \tau_0$ and τ_α are related

by the following relation:

$$\tau_\alpha = [t_c^{-n}\tau_0]^{1/(1-n)} \tag{1}$$

where $t_c = 2$ ps and n is the coupling parameter, which is related to the stretching of KWW function reproducing the structural peak, $n = 1 - \beta_{KWW}$, and it is usually considered a measure of the intermolecular coupling. According to the CM, a close relation is expected between timescales of slow (τ_α) and fast (τ_{JG}) relaxation and the dispersion of structural dynamics (β_{KWW}). The intermolecular coupling (n) is higher and the timescale separation of the JG peak from the structural one is larger, i.e. τ_α/τ_{JG}. Moreover, this relation is also expected to hold at different T and P. In fact, from equation (1), if $\tau_\alpha(T, P)$ is chosen constant for different combinations of T and P, then the stretching parameter β_{KWW} (and so n) is constant [14]; consequently τ_{JG} is also constant.

The aim of this paper is to show new experimental results on different glass-formers (low molecular glass-forming neat systems and binary mixtures) over a wide range of temperature and pressure, providing clear evidence that a strong correlation between slow (α-) and fast (JG β-) dynamics exists. Moreover, the dispersion of the structural relaxation will also be investigated, showing that if it varies over the investigated range, it remains unchanged for largely different combinations of T and P, once τ_α is fixed.

2. Experimental details

Diphenyl-vinylene carbonate (DPVC) was obtained from Aldrich. Its molecular weight is 348.15 g mol^{-1} and its glass-transition temperature, T_g, is 251 K. Benzoin-isobutylether (BIBE), obtained from Aldrich, was purified by distillation following the procedure illustrated in [17]. Its molecular weight is 268 g mol^{-1} and its T_g is 220 K. Quinaldine (QN, molecular weight 143.19 g mol^{-1}), and Tristyrene (3Styr, molecular weight 370 g mol^{-1}) were obtained from Aldrich and PSS, respectively, and used as received. The glass transition temperatures of pure QN molecules and 3Styr systems are 180 and 232 K, respectively. Dielectric measurements, both at atmospheric and at high pressure, were carried out using a Novocontrol alpha-analyser ($\nu = 10^{-5}$–10^7 Hz). For atmospheric pressure measurements, a parallel plate capacitor separated by a quartz spacer (geometric capacitance ∼90 pF) and filled by the sample was placed in the nitrogen flow Quatro cryostat. For high-pressure measurements, a sample-holder multilayer capacitor (geometric capacitance ∼30 pF) was isolated from the pressurizing fluid (silicon oil) by a Teflon membrane. Additionally, a simple parallel plate capacitor with Teflon spacers and Teflon support was also used for comparison. The dielectric cell was then placed in a Cu–Be alloy high-pressure chamber, provided by UNIPRESS, connected to a manually operated pump with a pressure intensifier able to reach 700 MPa. The high-pressure chamber was surrounded by a metallic jacket, whose temperature was varied in the interval 200–360 K and controlled within 0.1 K by means of a thermally conditioned liquid flow.

3. Results and discussion

3.1. Effect of temperature and pressure on structural α-relaxation and excess wing

DPVC is a quite rigid polar molecule that can be easily supercooled or overcompressed. Following a suitable cooling or compression rate, the crystallization can be avoided and a glass can be formed. Selected loss spectra of DPVC are shown in figure 1 from two different isobaric and isothermal paths. The α-peak can be well represented by the Fourier transform of the KWW function: the peak is quite narrow (β_{KWW} is not so far from 1), very similar to that of propylene

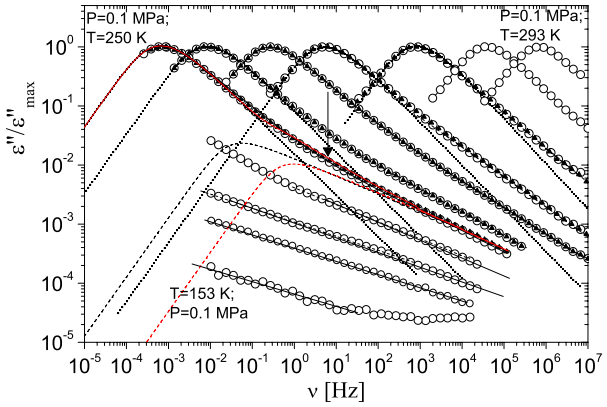

Figure 1. Normalized loss spectra of DPVC. Symbols represent experimental data: open circles from atmospheric pressure data (from right to left: 293, 283, 273, 263, 258, 253, 250, 243, 233, 193, 153 K), solid triangles are from high-pressure data at isotherm $T = 281$ K (from right to left: 36.5, 95, 126, 163, 190 MPa). Dotted lines are from fitting the KWW function ($\beta_{\mathrm{KWW}} = 0.77$, 0.73, 0.71, 0.70 from right to left). Dashed lines are from fitting the excess wing by a power-law or Cole–Davidson (CD) function. The continuous line is from fitting the total contribution. Red continuous and dashed lines are from a fit of the CD function with an alternative choice of fitting parameters (smaller $\Delta\varepsilon$ and shorter τ). The vertical line shows the frequency related to the primitive relaxation of the CM for the spectrum at 250 K and 0.1 MPa.

carbonate. As in the latter system, for DPVC, no well-resolved secondary β-processes are visible either in supercooled or in glassy state: instead an extra loss contribution (called the excess wing, EW) to the high-frequency side of the α-peak exists. It can be represented as a power law with a less steep slope than that characterizing the high-frequency side of the structural peak (see dashed lines in figure 1). The slope is decreasing with T. Concerning the microscopic origin of the EW, some authors proposed the EW as an inherent part of the α-relaxation [18, 19]. In contrast, recent experimental results suggested that the EW is nothing but the high-frequency side of a JG peak submerged by the structural one and closely connected to it: the EW was observed to transform into a resolved JG peak after ageing below T_{g} [20, 21] or at high pressure [22], and in a binary mixture after mixing with a higher T_{g} component [23]. The spectra in figure 1 were fitted with a superposition of the one-side Fourier transform of the KWW function for the structural peak and a Cole–Davidson (CD) function for the EW, although this procedure, already previously adopted in the literature [20], is somehow arbitrary. In fact, since in the spectra only the power law characterizing the high-frequency slope of the CD function can be clearly identified, one between the fitting parameters $\Delta\varepsilon$ and τ cannot be unambiguously determined. Different alternative sets of fitting parameters are possible, with a maximum frequency of the 'hidden' peak that can vary up to 2–3 orders of magnitude. An example is shown in figure 1. Moreover, different results can be obtained when two relaxation processes are so close in timescale, depending on the different deconvolution approaches used to describe the two processes, like, for example, the superposition or the Williams ansatz [25]. According to the last one, for example, the β-process shows up in the frequency domain as convoluted to the α-process, and so the maximum frequency of this 'effective' peak can be even two decades smaller than that expected for the 'pure' β-peak (see for instance figure 2 of [25]). For these reasons, any fitting procedure with a Cole–Davidson function to the excess wing has to be considered arbitrary.

It is much more interesting to compare the effect of isobaric cooling or isothermal compression on the whole dielectric response. The loss peak shifts to lower frequencies and

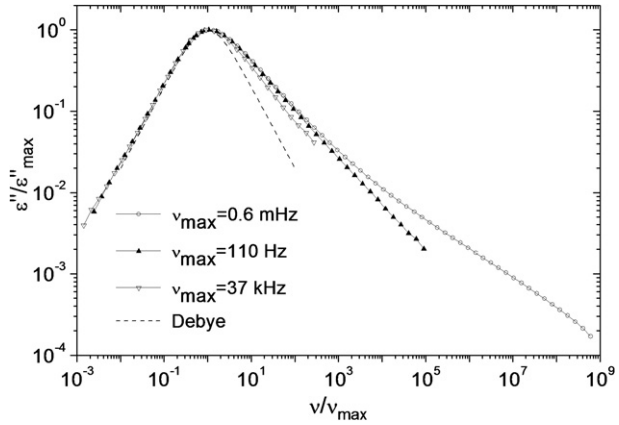

Figure 2. Comparison between selected spectra of DPVC at atmospheric pressure: dielectric losses normalized to the intensity of the maximum of the α-peak versus frequency normalized to the frequency of the maximum of the α-peak. Open triangles, solid triangles and open circles indicate spectra with $\nu_{\max} = 37$ kHz, 110 Hz and 0.6 mHz, respectively. Solid lines are guides for eyes; the dashed line is a Debye-like function.

the shape of the α-process as well as that of the excess wing change with T and P, but unexpectedly, spectra obtained in different T–P conditions but with the same peak-maximum frequency $\nu_{\alpha,\max}$ completely superpose over the wide frequency range measured. This result is not trivial, because the α-peak shape changes when τ_α increases, violating the so-called time–temperature-superposition principle, as shown in figure 2. The full width at half maximum (FWHM) changes from 1.39, 1.47 to 1.51, respectively, for 37 kHz, 110 Hz and 0.6 mHz (β_{KWW} goes from 0.77 to 0.70). Of particular interest is the fact that the violation is strongly evident in the region of the EW, but the same region is very well superposed when a comparison is done in figure 1 for spectra obtained at different T and P but with the same $\nu_{\alpha,\max}$. All these results prove that the EW and α-process are closely related and their dispersion and shape are determined by τ_α. If the explanation of the EW as an inherent part of the α-relaxation has to be rejected due to the evidences of [20–23], the results of figure 1 could be explained by assuming that the EW is an 'underlying' β-process whose timescale is affected by the pressure and is strongly correlated with α-relaxation.

In order to verify such a hypothesis, dielectric spectra of the small molecular glass-former BIBE have been analysed at different T and P, and a selection is shown in figure 3. BIBE has two secondary relaxations, one (γ-) intramolecular (faster) and one (JG β-) intermolecular (slower) relaxation [17]. The γ-process is almost insensitive to pressure and looks completely unrelated to the structural dynamics evolution, whereas the JG β-process shifts to lower frequency on applying moderate pressure (a few hundred MPa), following the α-peak. The loss spectra were fitted with a superposition of the Fourier transform of the KWW function for the α-process plus a Cole–Cole (CC) function $1/[1 + (\mathrm{j}\omega\tau)^{\delta}]$ for the JG relaxation. When τ_α is quite short, the α- and the JG processes are not well separated and an apparent EW scenario occurs as in the case of DPVC, but below T_{g} (or P_{g}) the JG β-peak becomes clearly visible. Moreover, as for the case of DPVC and the general rule of [14], a perfect superposition is obtained for a comparison of two spectra measured at different T and P but with the same $\nu_{\alpha,\max}(T, P)$, although the width of the α-peak changes for different $\nu_{\alpha,\max}$ (see figure 4). Furthermore, for constant $\nu_{\alpha,\max}(T, P)$, the timescale location of the JG process is also determined, although a perfect superposition can be attained, due to the difference of relative strength of the JG

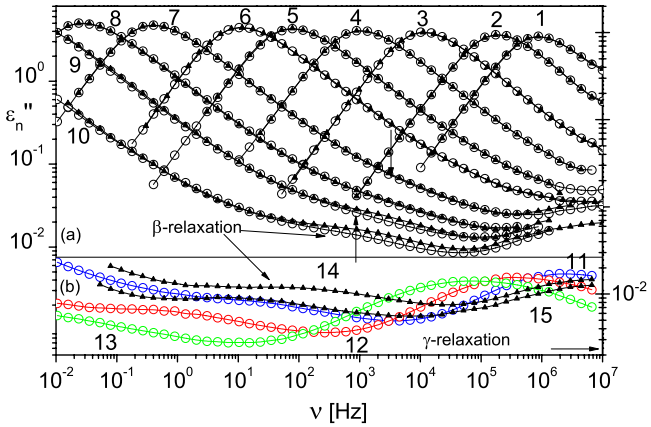

Figure 3. Dielectric loss of BIBE at different T and P. From right to left: open circles are atmospheric pressure data at $T = 271$ (1), 263 (2), 253 (3), 246 (4), 240 (5), 236 (6), 230 (7), 226 (8), 223 (9), 218 (10) and, in the lower panel, 205 (11—blue), 185 (12—red), 163 (13—green) K. Solid triangles are isothermal data at $T = 278.5$ K and pressure $P = 32$ (1), 65 (2), 120 (3), 204 (5), 225 (6), 283 (7), 320 (8), 350 (9), 395 (10) MPa and, in lower panel, at 288 K and $P = 516$ (14) and (15) 650 MPa. Vertical arrows indicate the frequency location of primitive relaxation for spectra (7) and (9).

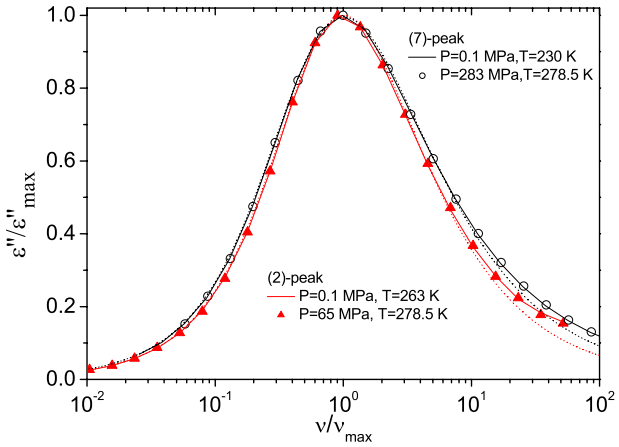

Figure 4. Comparison between spectra 2 ($\nu_{max} = 172$ kHz) and 7 ($\nu_{max} = 0.38$ Hz) from figure 3: data and fits are represented by symbols and lines in red and black colours, respectively. Dielectric losses normalized to the intensity of the maximum of the α-peak versus frequency normalized to the frequency of the maximum of the α-peak. Symbols indicate high-pressure data, solid lines indicate atmospheric-pressure data. Dotted lines are KWW fitting curves with $\beta_{KWW} = 0.78$ and 0.71, for spectra (2) and (7) respectively.

relaxation. The results found for BIBE and DPVC can be summarized thus: (i) the shape of the α-relaxation is determined only by the timescale τ_α, i.e. $\beta_{KWW}(\tau_\alpha)$; (ii) for a given combination of T_i and P_i so that $\tau_\alpha(T_i, P_i)$ is constant, also the JG relaxation time has a constant value $\tau_{JG}(T_i, P_i)$. The point (ii) is not trivially expected, as in figure 4 some spectra are well superposed, with a difference in T of almost 50 K. In fact, the JG β-relaxation (or the EW) appears to be strongly related to the structural one (although its P–T dependence is different) and to be quite sensitive to pressure. All these results can be rationalized by the CM:

in fact, the time of the primitive relaxation time τ_0, calculated from equation (1), agrees well with the JG relaxation time that can be found for our system (see the arrows in figure 3). For the case of DPVC, as the α-peak is quite narrow and $n = 1 - \beta_{\mathrm{KWW}}$ is quite small (0.29 at T_{g}), it follows that JG and α-process are not so well separated and the former appears as an EW. Moreover, as $n = 1 - \beta_{\mathrm{KWW}}$ is a function of τ_α, equation (1) also explains why τ_{JG} is a function only of τ_α, and it is also perfectly correlated for different combinations of T and P, provided that τ_α is constant.

3.2. Effect of temperature and pressure on genuine Johari–Goldstein β-relaxation

The results shown in the previous subsection are clear but the study carried on those systems has some drawbacks. First, the α- and β-processes are so close to each other in timescales that a quantitative analysis is not possible without using deconvolution or fitting procedures, thus introducing some bias. Moreover, especially for flexible systems with a multiple relaxation scenario (like BIBE), some objections could be raised about the nature of genuine JG relaxation for the observed β-process. For this reason, the same analysis along isobaric cooling and isothermal compression will be now shown for the binary mixture 5 wt% of QN in 3Styr. The components are both small molecules. QN is a quite rigid molecule, and as a neat system exhibits a dielectric response with no visible β-peak (but with an EW). After mixing with the less mobile molecules of 3Styr (3Styr has a T_{g} value 50 K higher than that of QN), the EW evolves in a well-resolved β-peak, more separated in timescale from the α-peak the higher is the concentration of 3Styr molecules, as previously observed in similar systems [23]. As the molecular dipole moment of QN and 3Styr is 3.8 and 0.2 D, respectively, the contribution of motions of QN dipoles to the dielectric response is dominant also at lower concentration of QN. A low QN concentration mixture has two main advantages: first, the α- and β-peaks are well separated and, secondly, the broadening of the structural peak due to concentration fluctuations should be not so important, allowing one to estimate the true coupling parameter n directly from the shape parameter β_{KWW}. In this way, a quantitative check of the prediction of the CM is possible and, moreover, a direct and unbiased test of the correlation between τ_{JG} and τ_α over T and P is possible. Examples of spectra obtained at atmospheric and high pressure for QN/3Styr (5%) are shown in figure 5. Also in this system, the width of the α-peak was found to be constant at constant τ_α value: in particular n was found to be 0.53 close to T_{g}. Calculating the frequency location of the primitive relaxation from equation (1), it was found to be close to the location of the β-process (see the arrows in figure 5). The dielectric spectra of the mixture QN/3Styr (5%) for isobaric cooling at $P = 0.1$ MPa and for isothermal compression at $T = 253$ and 300 K were fitted with a superposition of Fourier-transformed KWW function for structural relaxation and CC function for JG relaxation. Then, the most probable time $\tau = 1/(2\pi\nu_{\mathrm{max}})$ was calculated for both processes and the results are displayed in figure 6. Isobaric cooling data show a Vogel–Fulcher–Tammann (VFT) law for the α-relaxation time $\tau_\alpha = \tau_\infty \exp[B/(T - T_0)]$, and an Arrhenius behaviour for β-relaxation time τ_β with activation energy 54 ± 2 kJ mol^{-1} in the glassy state, but with a clear deviation (larger than the error bars) from this behaviour above T_{g}. The deviation is not due to fitting artefacts, because the large separation of the two processes (almost 7 decades) minimizes the effects of deconvolution procedures. Anyway, a similar deviation at T_{g} has been found also in [23], where a different procedure from our case was used to fit the data. Similarly, both sets of isothermal compression data show a much steeper pressure dependence for τ_α than τ_β, with a linear and steeper ($T = 253$ K) and slightly nonlinear ($T = 300$ K) law, following the empirical law $\tau_\alpha = \tau_\infty \exp[CP/(P_0 - P)]$ [24]. Concerning $\log_{10}(\tau_\beta)$, it has a linear behaviour versus P in the supercooled regime but it shows a kink corresponding to the glass transition pressure,

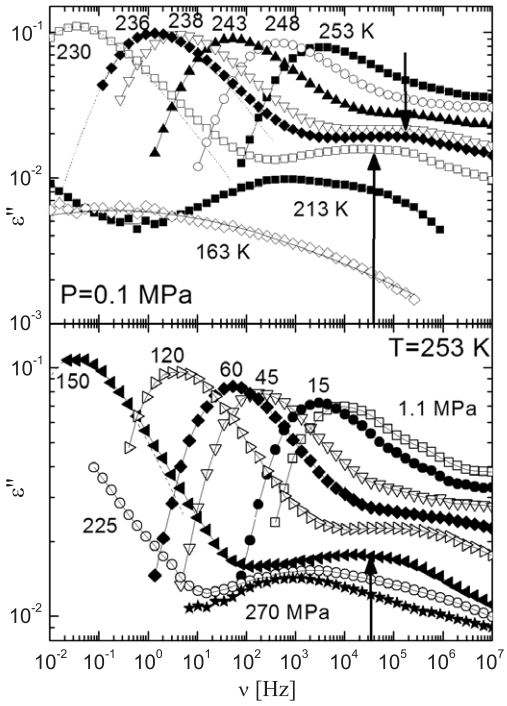

Figure 5. Log–log plot of selected dielectric loss spectra of the mixture QN/3Styr (5 wt%) versus frequency at atmospheric pressure at different temperatures (upper panel) and at high pressure at $T = 253$ K (lower panel). The low-frequency part of some spectra has been omitted for clarity. Symbols are experimental data, continuous lines are Havriliak–Negami fitting curves [27], and dotted lines are KWW function curves with $n = 0.53$. Vertical arrows indicate the locations of the calculated frequency ν_0 of the primitive process.

P_g, for both isotherms. The kink, that resembles the same transition for the isobaric relaxation map (figure 6(a)), is more evident for the isotherm at 253 K, where there can be observed a transition to another slightly linear regime in the glassy state, less steep, as expected, due the lower compressibility of the system in the glassy than the liquid state. Moreover, it has to be pointed out that the value of $\log_{10}(\tau_\beta)$ at the glass transition, i.e., when $\log_{10}(\tau_\alpha) = 2$, is almost the same (nearly -5) for the three set of data. It is noteworthy that the whole scenario shown for $\log_{10}(\tau_\beta)$ cannot be easily interpreted in terms of volume or density reduction. In fact, for our system, the glass transition for the three paths investigated occurs at different temperatures T_i, pressures P_i and volumes V_i, whereas all the dynamic features (i.e. the kink for $\log_{10}(\tau_\beta)$ versus P at P_g, the deviation from the Arrhenius behaviour of $\log_{10}(\tau_\beta)$ versus $1000/T$ at T_g, the constant location of $\log_{10}(\tau_\beta)$ when $\log_{10}(\tau_\alpha)$ is 2) occur at a given $\tau_\alpha(T_i, P_i)$. On the other hand, equation (1) of the CM can rationalize the results: as n has been found constant close to T_g, once τ_α is fixed, $\tau_0 \approx \tau_{JG}$ are also determined, irrespective of the vales of T and P. In particular, the calculated τ_0 is in agreement (within the error bars) with τ_{JG} of the observed JG relaxation (see figure 6).

4. Conclusions

The use of high-pressure dielectric measurements can single out and identify the JG β-relaxation. Performing measurements along different isobaric cooling and isothermal

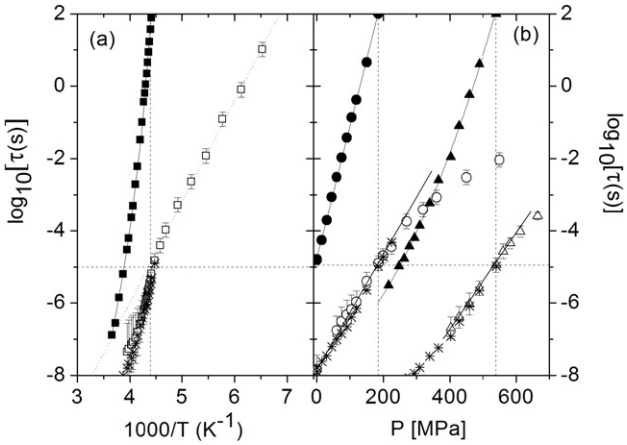

Figure 6. Relaxation map for the mixture QN/3Styr (5 wt%): (a) isobaric cooling at atmospheric pressure: logarithm of relaxation time (square symbols) versus $1000/T$; (b) isothermal compression at $T = 253$ K (circles) and $T = 300$ K (triangles). Solid and open symbols indicate α- and β-relaxation times, respectively. Continuous lines represent the VFT equation or the VFT-like equation for pressure data. The dotted line is the Arrhenius fit of β-relaxation time data at 0.1 MPa in the glassy state. Asterisks are the values of the calculated relaxation time τ_0 of the primitive process. Vertical dashed lines mark the location of the glass transition at different isobaric and isothermal conditions; the corresponding location of the β-relaxation time is indicated by the horizontal dashed lines.

compressing paths can allow one to check the correlation of the observed relaxations at different timescales. For the neat glass-formers DPVC and BIBE, a particular correlation has been found between the structural relaxation time τ_α, the dispersion of this process and the T–P dependence of the β-process, both when it is well resolved and when it is hidden as an EW process. The shape of the overall response (including the EW or β-process) is dependent only on the timescale of structural relaxation, independent of the particular values of T and P. For the binary mixture of 5 wt% QN in 3Styr, a model system for a genuine Johari–Goldstein relaxation, the qualitative evidences found on the neat systems were confirmed in a quantitative way. The primitive time of the CM was found to be in good agreement with the JG relaxation time. As the shape for this system is invariant, a constant ratio τ_α/τ_β was found at the glass transition (conventionally reached when $\log_{10}(\tau_\alpha) = 2$), irrespective of the T_g–P_g conditions chosen. A quite universal scenario appears: the local and fast β-process is correlated to the slow and cooperative α-process and this correlation is not lost when a reduction of volume occurs, provided that an increase of temperature will keep the τ_α constant. New experiments are needed to check if this simple picture (invariance of the α-shape and α–β separation for constant τ_α) will also hold for very strong reduction of volume, when the applied pressure approaches the value of the bulk modulus of the material.

Acknowledgments

The authors thank S Sharifi for assistance in dielectric measurements at high pressure. Financial support by MIUR-COFIN 2005 and by MIUR-FIRB 2003 (D.D.2186, grant RBNE03R78E) is gratefully acknowledged.

References

[1] Ngai K L, Casalini R, Capaccioli S, Paluch M and Roland C M 2006 *Advances in Chemical Physics* vol 133, part B *Fractals, Diffusion and Relaxation in Disordered Complex Systems* ed Y P Kalmykov, W T Coffey and S A Rice (New York: Wiley) chapter 10 p 497

[2] Johari G P and Goldstein M 1970 *J. Chem. Phys.* **53** 2372
Johari G P and Goldstein M 1972 *J. Chem. Phys.* **56** 4411
Johari G P 1973 *J. Chem. Phys.* **58** 1766

[3] Ngai K L and Paluch M 2004 *J. Chem. Phys.* **120** 857

[4] Ngai K L 1998 *J. Chem. Phys.* **109** 6982

[5] Ngai K L and Capaccioli S 2004 *Phys. Rev.* E **69** 031501

[6] Cohen M H and Grest G S 1979 *Phys. Rev.* B **20** 1077

[7] Adam G and Gibbs J H 1965 *J. Chem. Phys.* **43** 139

[8] Dlubek G *et al* 2005 *Macromolecules* **38** 429

[9] Prevosto D, Lucchesi M, Capaccioli S, Casalini R and Rolla P A 2003 *Phys. Rev.* B **67** 174202

[10] Casalini R and Roland C M 2004 *Phys. Rev.* E **69** 062501

[11] Alba-Simionesco C, Calliaux A, Alegria A and Tarjus G 2004 *Europhys. Lett.* **68** 58

[12] Casalini R, Roland C M and Mohanty U 2006 *J. Chem. Phys.* **125** 014505

[13] Böhmer R, Diezemann G, Geil B, Hinze G, Nowaczyk A and Winterlich M 2006 *Phys. Rev. Lett.* **67** 135701

[14] Ngai K L, Casalini R, Capaccioli S, Paluch M and Roland C M 2005 *J. Phys. Chem.* B **109** 17356

[15] Ngai K L 1979 *Comment. Solid State Phys.* **9** 127

[16] Ngai K L 2003 *J. Phys.: Condens. Matter* **15** S1107

[17] Kahle S, Schröter K, Hempel E and Donth E 1999 *J. Chem. Phys.* **111** 6462

[18] Dixon P K, Wu L, Nagel S R, Williams B D and Carini J P 1990 *Phys. Rev. Lett.* **65** 1108

[19] Chamberlin R V 1993 *Phys. Rev.* B **48** 15638

[20] Schneider U, Brand R, Lunkenheimer P and Loidl A 2000 *Phys. Rev. Lett.* **84** 5560

[21] Ngai K L, Lunkenheimer P, Leon C, Schneider U, Brand R and Loidl A 2001 *J. Chem. Phys.* **115** 1405

[22] Casalini R and Roland C M 2003 *Phys. Rev. Lett.* **91** 015702

[23] Blochowicz T and Rössler E A 2004 *Phys. Rev. Lett.* **92** 225701

[24] Corezzi S, Rolla P A, Paluch M, Zioło J and Fioretto D 1999 *Phys. Rev.* E **60** 4444

[25] Svanberg C, Bergman R and Jacobsson P 2003 *Europhys. Lett.* **64** 358

[26] Kudlik A, Tschirwitz C, Benkhof S, Blochowicz T and Rössler E 1997 *Europhys. Lett.* **40** 649

[27] Garwe F, Schönhals A, Lockwenz H, Beiner M, Schröter K and Donth E 1996 *Macromolecules* **29** 247

[28] Wagner H and Richert R 1999 *J. Phys. Chem.* B **103** 4071